Astron. Astrophys. 334, L77–L80 (1998)

ASTRONOMY AND ASTROPHYSICS

LETTER

Letter to the Editor

Observational evidence for coronal mass injection by "evaporation" of spicular plasma

F. Budnik[1], **K.-P. Schröder**[2], **K. Wilhelm**[3], **and K.-H. Glassmeier**[1]

[1] Institut für Geophysik und Meteorologie, Mendelssohnstrasse 3, D-38106 Braunschweig, Germany
[2] Institut für Astronomie und Astrophysik, Hardenbergstrasse 36 (PN 8-1), D-10623 Berlin, Germany
[3] Max-Planck-Institut für Aeronomie, D-37189 Katlenburg-Lindau, Germany

Received 16 March 1998 / Accepted 28 April 1998

Abstract. Despite being a common feature of the solar chromosphere, spicules are still a poorly understood phenomenon. Not much is known about their impact on the physics of the transition region and corona, for which spicules are believed to be the dominant mechanism for mass injection. We recently observed the spatial plasma structure of polar spicules in a large temperature range with the EUV spectrometer SUMER onboard the SOHO spacecraft. The spectrometer slit was placed tangentially to the polar limb at various projected heights $< 22''$. Our spectra in the wavelength range of 748–792 Å simultaneously record emission lines which are formed in a wide temperature range between 30 000 and 600 000 K.We find that the typical structure of spicular plasma grows, horizontally and vertically, with increasing emission-line temperature, reaching $\approx 20''$ at $1 - 2 \cdot 10^5$ K. This suggests an "evaporation" of spicular plasma into the transition region (TR) and corona, for which we find further evidence from an emission measure analysis.

Key words: Sun: spicules – atmosphere – chromosphere – transition region – UV radiation

1. Introduction

Solar spicules have been observed for more than a century. They are known to be chromospheric material ejected at velocities of typically 25 km/s. They reach heights of 10 000–15 000 km, when observed in H_α, and their diameters are of the order of 1 000 km. A comprehensive review of spicular properties is given by Beckers (1972). Several models have been suggested in which plasma is accelerated inside a flux-tube to form well collimated, jet-like spicules. However, it is still not clear, what physical processes the main drivers for spicules are. See, e.g., Lorrain & Koutchmy (1996) and Cheng (1992) for different approaches.

Send offprint requests to: F. Budnik
(e-mail: frank@geophys.nat.tu-bs.de)

The globally averaged spicular mass-flux exceeds the coronal mass-loss rate by roughly a factor of hundred (Pneuman & Kopp 1977). Hence, although being a minor factor in the coronal energy balance, spicules can well provide the main mass injection rate for the corona, even if most of the spicular material falls back into the chromosphere and only $\approx$ 1% of it would "evaporate".

In fact, spicular structure is observed in the same EUV lines as is the TR (e.g., Dere et al. 1983), which immediately suggests that some spicular plasma is indeed heated up to $\gtrsim 10^5$ K. This has also been confirmed from theoretical modeling (Cheng 1992). However, an alternative interpretation has been suggested: rather than being a static, flat layer, the TR might adjust itself to dynamically surround rising cool spicules. Consequently, any observed EUV emission could just come from such a TR envelope of a spicule (Mariska et al. 1978; Withbroe 1983), rather than from some hotter plasma of the spicule itself.

An average redshifted UV line emission from plasma of $\approx 10^5$ K indicates the presence of downflows in the solar TR (e.g. Brekke et al. 1997; Chae et al. 1998). It has been suggested that heated spicular plasma, falling back to the chromosphere, could account for those redshifts (Pneuman & Kopp 1977). Similar line redshifts have also been reported from stellar TR line observations of many solar-like stars (e.g., Ayres et al. 1983, Ayres et al. 1988), outlining the general character of this problem. Nevertheless, it has remained unclear, whether evaporating spicular plasma is actually re-substituting solar and stellar coronal mass-losses.

We have studied the spatial structure of spicular plasma over the solar limb at different temperatures to look for evidence that spicular plasma is disintegrated or "evaporated" into the corona.

2. Observations

SUMER (Solar Ultraviolet Measurements of Emitted Radiation) is a stigmatic, high resolution normal-incidence spectrograph onboard the SOHO spacecraft. With a spatial resolution element of $1''$(725 km on the Sun), and a spectral coverage of 465 to 1610 Å, it has been designed to investigate the physics

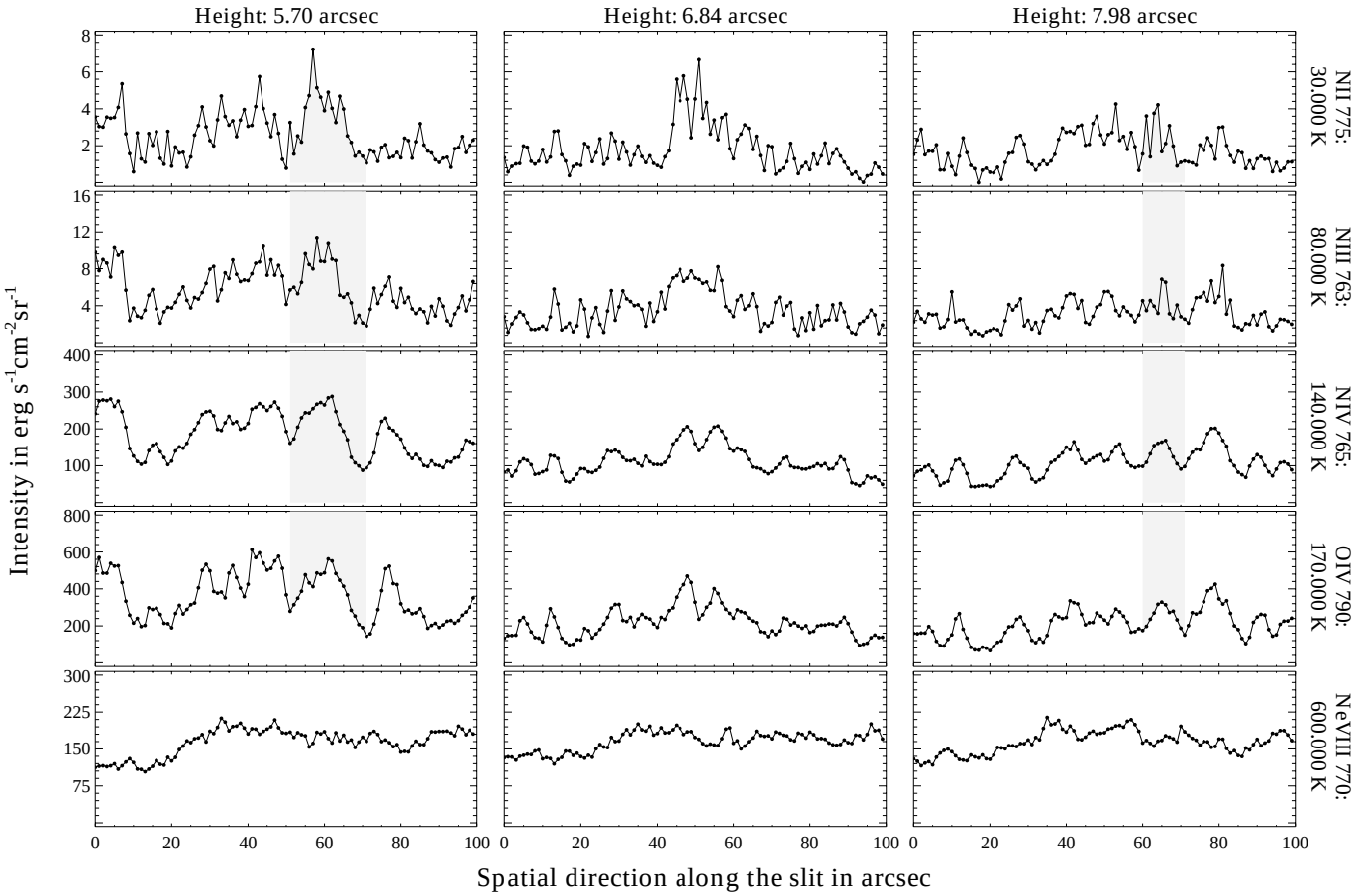

Fig. 1. The spatial variation along the slit of wavelength-integrated emission line intensity is shown for five ions at three projected heights above the northern white-light limb. Wavelengths and emission line temperatures are indicated at the right side. The grey shaded regions highlight the features selected for Table 1.

of solar fine structure in the EUV. For a detailed description of the instrument see Wilhelm et al. (1995).

A 90° roll maneuver of SOHO has been used to place the 1x120 arcsec^2 slit tangentially to the north polar limb, where the fewer but larger polar spicules offer a better chance to study individual features than near the solar equator. Spectra have been taken at various projected heights between 0 and 22″ above the white light limb, with a step size of 1.″14. On the west end of the slit, about 19″ have been cut off because the slit image was not fully aligned with the read-out window of the detector. Due to the Sun's curvature, the slit-end heights above the white-light limb are larger by about 1.″7 or 1 250 km (east end) and 0.″8 or 550 km (west end).

All spectra were obtained with the SUMER detector B and an exposure time of 45 s. The selected wavelength range of 748 to 792 Å shows various emission lines (see below) which represent a wide temperature range, including emission from the TR and lower corona. Three spectra have been taken at each height step, which required approximately 3 min observing time each. Thus, we can test the dynamical time-scale of spicules at each height, but spicular life-times are already exceeded after about 2 height steps.

Several data reduction steps have been applied to the SUMER raw data, i.e., flat-field correction (using an onboard-exposure taken three weeks prior to the observations), instrumental line curvature (by SUMER software) and intensity calibration (based on the pre-launch radiometric calibration of Hollandt et al. 1996).

Fig. 1 shows the spatial variation (along the slit) of five selected, wavelength-integrated line intensities for three selected height steps, which represent the best compromise between line-of-sight confusion of individual features and signal-to-noise ratio (particularly critical with the N II 775 and N III 763 lines), both decreasing with increasing height. Count statistics have shown that the major features in the N II/N III emission lines are well above the statistical noise. The chosen emission lines are unaffected by blends, and the intensities shown have been obtained by a simple integration over the full line width, after subtracting the apparent continuum. Each temperature of maximum contribution ($G(T)$, see below) is indicated, ordered to increase from top to bottom. N II 775 and N III 763 represent temperatures of the lower TR, N IV 765 and O IV 790 are associated with the TR, and Ne VIII 770, the hottest emission, is a typical line of the lower corona. The time differences between

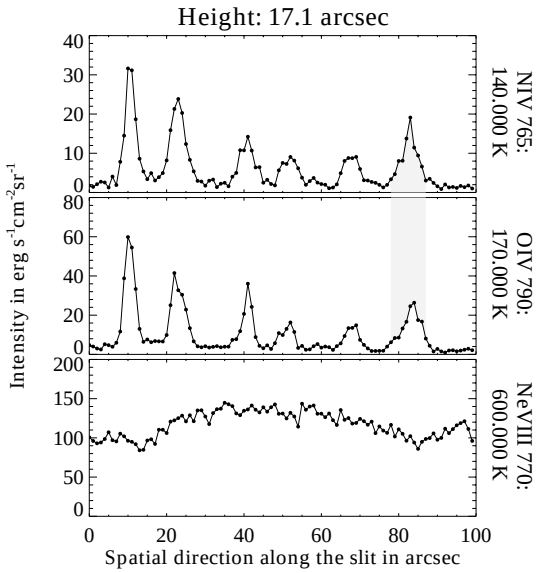

Fig. 2. Spatial variation of the integrated line intensities at 17″.1 above the white light limb: N IV, O IV and Ne VIII – compare to Fig. 1.

the second and third column to the first height step shown is 10 and 16 min, respectively.

Fixed intensity scales have been used in Fig. 1 to demonstrate the decrease of intensity with increasing projected height. This is true for the emission of all ions, except for Ne VIII. Sharp spicular structures can easily be seen in the N II and N III line intensities. At heights of 5″.7 to 6″.84 the spicular widths appear to be close to the instrumental spatial resolution, somewhere between 1″ and 3″, similar to spicules observed in H_α.

By contrast, the N IV and O IV lines, emitted by plasma of about 140 000 K and 170 000 K, respectively, exhibit a much more diffuse structure. Observed widths range from 5″ to 20″. Each feature seems to coincide with a bunch of spicules, seen sharply in the N II and N III emission lines, or at least one prominent spicule.

By contrast, no defined features can be found in the coronal Ne VIII emission line, which is emitted by plasma at temperatures around 600 000 K, that is, any features seen at lower temperatures seems to be fully disintegrated at coronal temperatures. This is consistent with other EUV observations (see Withbroe 1983).

Not only the spatial coincidence of the broad N IV/O IV features with, mostly, bunches of sharp N II/N III spicules suggests that we actually see plasma of spicular origin at some 10^5 K. Further evidence comes from the dynamical time-scales: While individual N II/N III spicules have life-times of about our time resolution (3 min, see above), most N IV/O IV features last about 10 min, what would be the expected dynamical time-scale of a bunch of spicules.

Fig. 2 shows the even clearer spatial variation of the integrated N IV 765, O IV 790 line intensity at a *large* projected height, 17″.1 above the limb – compare to Fig. 1. We observe a pronounced structure with a spatial extent of about 10″, while the sharp, cool plasma features (N II and N III lines) do not extend to those heights. Some regularity might suggest an interpretation as polar plumes. But, again, the dynamic time-scale is short of 10 min and the hot coronal Ne VIII 770 line is featureless, while polar plumes are known to be of long duration (tens of hours) and are visible in coronal lines.

We interpret these N IV/O IV features as spicular plasma which is heated up to $\gtrsim 10^5$ K, expands and then disintegrates – say: "evaporates" into the lower corona. Further evidence comes from a first quantitative interpretation of our data as given below.

3. Emission measure analysis

In order to derive an estimate of the relative plasma quantities observed in the various temperature ranges, we carried out an emission measure analysis for selected spicular features.

The total intensity I (in erg s^{-1} cm^{-2}sr^{-1}) emitted by an optically thin plasma, in an emission line of wavelength λ and integrated over the line of sight, is given by:

$$I(\lambda) = \frac{1}{4\pi}\frac{hc}{\lambda}\int_{LOS} G(T)N_e^2 ds \quad . \tag{1}$$

$G(T)$ is the strongly temperature dependent contribution function which includes the ionisation ratio, the relative element abundance and several atomic parameter. We assume local ionisation equilibrium and adopted the ionisation ratios from Arnaud & Rothenflug (1985). The element abundances are taken from Feldman et al. (1992). For temperatures larger than 20 000 K, the ratio of hydrogen density to the electron density N_e is set to 0.8. The CHIANTI atomic database (Dere et al. 1997) has been used for the calculation of $G(T)$.

In order to simplify Eq. (1), we substitute the spicular electron density by a constant average of N_e and assume that the major contribution to the emitted intensity comes from plasma with a temperature near maximum $G(T)$ ($T_{\max}$). We then follow a procedure used by Mariska (1980) and compute a $< G(T_{\max}) >$, i.e. we average $G(T)$ over a 0.2 dex interval centered on log$T_{\max}$, and Eq. (1) reads:

$$I(\lambda) = \frac{1}{4\pi}\frac{hc}{\lambda} < G(T) > \left(N_e^2 \Delta s\right) \quad . \tag{2}$$

That links $N_e^2\Delta s$, the emission measure EM, directly to the observed, wavelength-integrated emission-line intensity. The reasonable assumption, that the line-of-sight extension Δs of the spicular plasma equals the observed width (725 km per 1″), yields an estimate of the electron density N_e – representive of the total plasma in the projected height of the slit and in each emission-line temperature.

That procedure has been applied to some of the larger features in Figs. 1 and 2 (shaded), after clearing their intensities from some back- and foreground emission. Table 1 summarizes some typical results. The chosen broad features in N IV and O IV are related to a bunch of sharp N II and N III spicules, each, of which always the brightest one has been measured. Spicules are known to come in bunches, but some N II and N III features may also be aligned by chance. Their Δs might well be overestimated, since the observed widths are near the resolution limit,

Table 1. Spatial extension and estimated spicular electron densities for different plasma temperatures

			$N_e/10^9$ cm^{-3}		
	$T_{\max}$/K	Total widths	Height: 5″.7	Height: 7″.98	Height: 17″.1
N II	$3{\cdot}10^4$	2″–3″	2.0	1.4	–
N III	$8{\cdot}10^4$	2″–3″	1.7	1.2	–
N IV	$1.4{\cdot}10^5$	10″–20″	1.2	1.0	0.32
O IV	$1.7{\cdot}10^5$	10″–20″	1.1	1.0	0.27

i.e. the electron densities derived from the N II and N III lines are only lower limits. Note that all densities are decreasing with increasing height and with increasing $T_{\max}$ of the emission lines.

4. Discussion and conclusions

The evidence presented here sheds new light on spicules and the TR. Further, simultaneous observations with the Izaña (Tenerife) solar observatory and SUMER are planned and will provide a larger spectral coverage and an even better spatial and temporal resolution. Prior to any more detailed analysis we can, nevertheless, draw some conclusions here:

The typical spatial extent of spicule-related features grows significantly with increasing plasma temperature until all defined features have disappeared at $6 \cdot 10^5$ K. Furthermore, estimated electron densities (see Table 1) fall between the 10^{11} cm^{-3} (Beckers 1972) of H_α spicules (representing the thermally stable spicular plasma of $\lesssim 10^4$ K) and typical densities of the corona. For 1 to $2{\cdot}10^5$ K, largest spicular plasma densities ($1.2 \cdot 10^9$ cm^{-3}) yield sufficient thermal gas pressure $P_g \propto N_e \cdot T_e$ (T_e is the electron temperature) to exceed the coronal gas pressure in magnetically open regions (assuming coronal densities of $\approx 10^8$ cm^{-3} at $\lesssim 10^6$ K). This is exactly what we should expect, once part of the cool spicular plasma has been heated beyond the Lyα-related radiative cooling peak and then expands into disintegration to re-substitute TR and coronal plasma.

The plasma in the features observed at 1 to $2{\cdot}10^5$ K clearly has a higher density than the TR plasma seen in the same lines-of-sight: we find that the maximum TR line intensity (at a height of $\approx 3''$, in erg s^{-1} cm^{-2} sr^{-1}: 180 (N IV), 300 (O IV)) does not exceed the typical background-corrected peak intensity of diffused spicular plasma features, although their extension in the line-of-sight is an order of magnitude smaller than that of the TR. Therefore, instantaneously heated (by e.g. internal shockwaves) spicular plasma itself is observed rather than a TR envelope – the latter would not yield sufficient contrast between individual features and the TR background.

Mostly, a whole bunch of spicules seems to form those diffuse plasma features. It is therefore not easy to quantify the evaporating fraction of spicular plasma – apparently 1 to 10% seems to be visible at TR temperatures. Considering the TR-lines average redshifts, part of that plasma must be flowing back into the chromosphere. However, its strong degree of spatial disintegration, its thermal instability (radiative cooling decreases with further increase of temperature) and its sufficiently large gas pressure, all that is strong evidence that evaporation of spicular plasma into the corona is actually happening.

Acknowledgements. The SUMER project is financially supported by DLR, CNES, NASA and the ESA PRODEX program (Swiss contribution). SUMER is part of SOHO, the *Solar and Heliospheric Observatory* of ESA and NASA. We want to thank W. Curdt and R. Bodmer for their support during the SUMER raw data analysis, and R. Hammer and S. Zidowitz for fruitful discussions.

References

Arnaud, M., Rothenflug, D., 1985, A&AS, 60, 425
Ayres, T.R., Stencel, R.E., Linsky, J.L., Simon, T., Jordan, C., Brown, A., Engvold, O., 1983, ApJ, 274, 801
Ayres, T.R., Jensen, E., Engvold, O., 1988, ApJS, 66, 51
Beckers, J.M., 1972, Ann. Rev. Astron. Astrophys., 10, 73
Brekke, P., Hassler, D.M., Wilhelm, K., 1997, Solar Phys., 175, 349
Chae, J. Yun, H.S., Poland, A.I., 1998, ApJS, 114, 151
Cheng, Q.-Q., 1992, A&A, 262, 581
Dere, K.P., Bartoe J.-D.F., Brueckner, G.E., 1983, ApJ, 267, L65
Dere, K.P., Landi, E., Mason, H.E., Monsignori Fossi, B.C., Young, P.R., 1997, A&AS, 125, 149
Feldman, U., 1992, Physica Scripta, 46, 202
Hollandt, J., Schühle, U., Paustian, W., Curdt, W. Kühne, M., Wende, B., and Wilhelm, K., 1996, Appl. Opt., 35, 5125
Lorrain, P., Koutchmy, S., 1996, Solar Phys., 165, 115
Mariska, J.T., 1980, ApJ, 235, 268
Mariska, J.T., Feldman, U., Doschek, G.A., 1978, ApJ, 226, 698
Pneuman, G.W., Kopp, R.A., 1978, Solar Phys., 57, 49
Wilhelm, K., Curdt, W., Marsch, E., Schühle, U., Lemaire, P., Gabriel, A., et al., 1995, Solar Phys., 162, 189
Withbroe, G.L., 1983, ApJ, 267, 825